Romanian Journal of Ecology & Environmental Chemistry, 7(2), 2025
https://doi.org/10.21698/rjeec.2025.206

Article

Impact of flooding on the multifunctionality of Glycyrrhiza uralensis: a comparative study of phytochemical, antioxidant, anticorrosion, and photoprotective activities

GAUHAR UZAKBAY, NIKOLAY AKATYEV*

Faculty of Natural and Geographical Sciences, M. Utemisov West Kazakhstan University, Uralsk, Kazakhstan
**Corresponding author: n.akatyev.science@gmail.com*

Received:	*Reviewed:*	*Accepted:*
25.11.2025	*03.12.2025*	*12.12.2025*

Abstract
This study provides a comprehensive assessment of the effects of severe flood stress on the phytochemical composition and multifunctional characteristics of Glycyrrhiza uralensis (Ural licorice). Aqueous extracts from different plant parts collected before (2023) and after flooding (2024) were analyzed using spectrophotometric and gravimetric methods to evaluate antioxidant capacity, sun protection potential, and corrosion inhibition efficiency. Flooding induced a pronounced metabolic reorganization, marked by a significant increase in total phenolic content (TPC) and a decrease in total flavonoid content (TFC), resulting in an elevated TPC/TFC ratio. These changes reflected the accumulation of more conjugated, redox-active phenolic structures with extended π-systems, enhancing both electron-donating ability and metal adsorption efficiency. Functionally, post-flood extracts exhibited higher antioxidant activity, greater photostability, and improved corrosion inhibition in both neutral and acidic media. Pearson correlation analysis (PCA) confirmed that TPC and TFC were the primary determinants of multifunctional performance, though partial correlation reversals indicated a redistribution of biochemical roles under stress. Research findings highlight flooding as a powerful biochemical modulator that increases Glycyrrhiza uralensis protection potential and provide valuable insights into how environmental extremes change plant metabolism for adaptive multifunctionality.

Keywords: *Glycyrrhiza uralensis, flooding, phytochemical composition, antioxidant activity, PCA*

INTRODUCTION

Glycyrrhiza uralensis, or Ural licorice, is a medicinally valuable species known for its broad range of biological activities. Its roots and rhizomes contain a complex mixture of pharmacologically active constituents—most notably triterpenoid saponins, flavonoids, and various polysaccharides—that underpin its therapeutic potential. Traditionally, the plant has been employed for its anti-inflammatory, antiviral, hepatoprotective, and antioxidant effects. Contemporary research has further demonstrated its relevance in anticancer therapy, infection control, and modulation of immune responses. In addition, compounds from *G. uralensis* have shown beneficial effects in models of neurodegenerative disorders, including Alzheimer's and Parkinson's diseases, largely through the suppression of oxidative stress and inhibition of amyloid formation. Its derivatives, such as glycyrrhizic acid, are also utilized in food, cosmetics, and fine chemicals, highlighting its versatility and importance in both medicine and industry [1,2].

G. uralensis holds an important place in the flora of Kazakhstan. It is an indigenous species occurring extensively throughout the steppe and semi-desert zones of the country. The plant thrives in saline soils, river valleys, and floodplains, making it well-adapted to Kazakhstan's arid and semi-arid climate. *G. uralensis* was studied at multiple sites in southeastern Kazakhstan and found that it coexists with *G. glabra*, forming mixed populations. HPLC profiling confirmed the presence of characteristic compounds unique to *G. uralensis*. New bioactive compounds, including licoleafol and uralstilbene, along with known flavonoids, were identified [3]. *G. uralensis*, which grows in the Western region of Kazakhstan, has been studied for the content of natural plant pigments. The

influence of the flood on their total and relative content was studied [4]. Thus, despite its prevalence and practical importance, and perspectives *G. uralensis* remains an almost unexplored plant.
Plant extracts with multifunctional properties have been extensively investigated in recent studies aiming to evaluate multiple beneficial activities simultaneously, particularly the combinations of antioxidant–photoprotective and antioxidant–anticorrosive effects. For antioxidant-sun protection combinations, Kurzawa *et al.* studied total phenolic content, antioxidant capacity, and UV protection properties across four plant extracts (marigold, carrot, tomato, hop), finding hop cones showed both highest phenolic content and high radiation protection [5]. Similarly, Nunes *et al.* evaluated sun protection factor in relation to antioxidant activity and phenolic content in Brazilian plant extracts [6]. Ferreira Júnior *et al.* evaluated phenolic- and amino-rich plant extracts from Northeastern Brazil, demonstrating a relationship between their corrosion-inhibiting ability and antiradical activity [7]. Vorobyova *et al.* provide a comprehensive review examining the correlation between antioxidant activity and anticorrosion properties across multiple plant extract studies [8].
The aim of this study is to assess the effect of flood stress on the phytochemical composition and multifunctional behaviour of extracts of *G. uralensis* from various parts of the plant collected in western Kazakhstan. By integrating spectrophotometric, gravimetric, and statistical approaches, the work sought to elucidate the mechanisms through which flooding modifies phytoconstituent profiles and, consequently, the antioxidant, photoprotective, and anticorrosive activities of the studied extracts.

MATERIALS AND METHODS

Reagents.

All reagents employed in this study were of analytical grade and sourced from commercial suppliers. They were utilized without any additional purification. All solution preparations and extraction processes were carried out using double-distilled water (DDW).

Collection, authentication, and preparation of plant material.

The plants were gathered during the flowering stage in the summer in natural habitats located at a distance from roads and industrial zones (51°10'43.6"N 51°22'24.7"E, Figure 1).

A **B**

Fig. 1. The place of collection of *G. uralensis* plant in 2023 (A) and 2024 (B).

Species identification was confirmed at the Herbarium of the Faculty of Natural and Geographical Sciences, M. Utemisov West Kazakhstan University. Prior to further processing, the plant materials were thoroughly cleaned to remove dust and sand by washing first with running water and subsequently with DDW. The washed samples were air-dried in a shaded, well-ventilated area under ambient conditions for approximately two weeks, until complete dehydration was achieved. The dried

plant material was finely milled, sieved through a 1.0-mm mesh, and stored at 4 °C for subsequent extraction procedures.

Extract preparation.

Extraction was performed by transferring 10 g of dried and milled plant sample into a 250 mL flask and conducting three successive extractions with 100 mL of DDW each for 4 hours at 60°C. The extracts were merged and concentrated by evaporating the remaining solvent. The remaining residue was then dried at 50°C and stored at 4°C until further use.

Qualitative phytochemical analysis.

The obtained aqueous extracts of *G.uralensis* were subjected to qualitative phytochemical tests using standard techniques [9÷11]. The presence of primary and secondary metabolites was determined.

Determination of total phenolic content (TPC)

TPC of the extracts was measured spectrophotometrically at 760 nm against blank using the Folin–Ciocalteu reagent according to the reported procedure [12]. TPC values were determined from standard gallic acid calibration curve (0-100 μg/mL, $y = 0.2484x - 0.2369$, $R^2 = 0.9993$) and expressed as mgGAE/g. The TPC in all samples was calculated the using following expression:

$$TPC=(CxV)/M \quad (1)$$

where, TPC – total phenolic content (mgGAE/g), C - concentration of gallic acid obtained from calibration curve in (mg/mL), V - volume of extract (mL), M - weight of extract in (g).

Determination of total flavonoid content (TFC)

The TFC of the extracts (expressed in mgQE) was measured using the aluminum chloride colorimetric assay at 510 nm against blank following the procedure reported by Zhishen *et al.* [13]. The standard curve ($y = 1.0571x - 0.0047$, $R^2 = 0.9995$) for total flavonoids was obtained using quercetin as a standard (0 to 1 mg/mL).

Total antioxidant capacity (TAC)

The TAC of the tested extracts (in mmol of ascorbic acid (AA)/g) was determined by the phosphomolybdate method at 765 nm against a blank [14].

Total reducing power (TRP)

TRP determination assay (in mmolAA/g) is based on the reduction of Fe^{3+} to Fe^{2+} by the extract's phytocomponents. The resulting Fe^{2+} was quantified by measuring the formation of Perl's Prussian blue at 700 nm [15].

DPPH (2,2-diphenyl-1-picrylhydrazyl) radical scavenging activity.

DPPH-radical scavenging activity was determined as described by Brand-Williams at 517 nm against methanol as a blank [16]. The ability of extracts to scavenge DPPH radical was calculated as follows:

$$\text{DPPH scavenging activity} = (A_0 - A_1)x100/A_0 \quad (2)$$

where, A_0 is the absorbance of the control, and A_1 is the absorbance of the extract or standard. Ascorbic acid at the same concentration range was used as positive control.

Hydrogen peroxide (H_2O_2) scavenging activity (HPSA)

The HPSA was estimated by the 1,10-phenanthroline method with ascorbic acid as a standard at 510 nm with a spectrophotometer against blank [17]. The HPSA percentage was calculated as follows:

$$HPSA=Abs_{sample}x100/Abs_{blank} \quad (3)$$

where Abs_{sample} are the absorbance of solution of extract (or standard), ferrous ammonium sulfate and hydrogen peroxide; Abs_{blank} is the absorbance of solution containing only Fe^{2+} - NH_4^+ sulphate, water and 1,10-phenanthroline. A blank reagent containing only 1,10-phenanthroline was also prepared.

Hydroxyl radical scavenging activity (HRSA)
Determination of HRSA was performed spectrophotometrically at 562 nm as described by Govindan [18]. The HRSA was calculated as follows:

$$HRSA\ (\%) = [1-(A_1-A_2)x100]/A_0 \quad (4)$$

where A_0 was the absorbance of the control (without extract), A_1 was the absorbance in the presence of the extract, and A_2 was the absorbance without sodium salicylate. Mannitol was used as a positive control [19].

Nitric oxide (NO) radical scavenging activity (NO•RSA)
NO•RSA was estimated spectrophotometrically using Griess reagent [20]. The absorbance of the formed chromophore was measured at 546 nm. The nitrite produced in the presence or absence of the plant extract was estimated using a standard curve ($y = 0.2104x - 0.0412$, $R^2 = 0.9993$) based on sodium nitrite solutions of known concentrations. Ascorbic acid was used as a standard. The percentage of inhibition was calculated using the following formula:

$$NO^{\bullet}\ scavenging\ effect\ (\%\ of\ inhibition) = (A_0 - A_1)x100/A_0 \quad (5)$$

where, A_0 is the absorbance of the control, and A_1 is the absorbance of the extract or standard. A control experiment was performed in the same way without test compound but with the equivalent amount of solvent.

Determination of the sun protection factor (SPF)
To determine the SPF, the dried extracts were dissolved in pure ethanol to obtain concentration of 1.0 mg/mL. The absorption spectra were recorded with a spectrophotometer in the UVB region (290 to 320 nm), with intervals of 5 nm, in a 1.0 cm quartz cuvette against pure solvent as a blank sample. The SPF values were calculated using the Mansur equation [21] as follows:

$$SPF = CF \sum_{290}^{320} EE(\lambda) \times I(\lambda) \times abs(\lambda) \quad (6)$$

where EE (λ) is the erythemal effect spectrum, I (λ) is the solar intensity spectrum, abs (λ) is the absorbance, CF is the correction factor (10). The values of EE x I are constants determined by Sayre *et al.* [22] and listed in Table 1.

Table 1. Normalized product function used in the calculation of SPF

Wavelength, nm	EE x I*
290	0.0150
295	0.0817
300	0.2874
305	0.3278
310	0.1864
315	0.0839
320	0.0180
Total	1.0000

*EE: erythemal effect spectrum; I: solar intensity spectrum

Determination of photostability (PS)
To investigate the photostability of the aqueous extracts of *G.uralensis*, the extract solutions were divided into two sets and stored parallelly in sunlight and in the dark for 6 weeks at room temperature. The photostability of tested extracts was calculated with the following equation:

$$PS\ (\%) = SPFx100/SPF_0 \quad (7)$$

where SPF_0 is the sun protection factor of freshly prepared extract, and SPF is the sun protection factor of extract after 6 weeks of exposition.

Determination of photosensitivity (ΔPS)
The value that characterizes the photosensitivity of an extract when exposed to sunlight was calculated as the difference between the sun protection factor (SPF) values of the extract measured after storage in sunlight and in the dark at the same exposure time, as follows [23]:

$$\Delta PS\ (\%) = PS_{dark} - PS_{sunlight} \quad (8)$$

where $PS_{sunlight}$ and PS_{dark} are SPF value measured after storage of the extract in sunlight and in the dark, respectively. The lower this value, the more photostable the extract is and less susceptible to sunlight.

Corrosion experiments
Carbon steel specimens (2.5 × 3.5 × 0.3 cm) with the chemical composition (wt%) of 97.8 (Fe), 0.22 (C), 0.65 (Mn), 0.30 (Si), 0.04 (P), 0.05 (S), 0.30 (Cr), 0.30 (Ni), 0.30 (Cu), 0.01 (N), and 0.08 (As) were sourced from industry. The metal surface was polished using 250-1200 grit emery paper and then was thoroughly cleaned with running water and DDW. The samples were then washed with ethanol and acetone, dried in air and stored under silica gel until being used for corrosion testing.

Weight loss assay
Each steel specimens was immersed in a beaker filled with 100 ml of corrosion medium at ambient temperature. After the immersion period, the coupons were removed from the beaker, rinsed with running water and DDW, and then cleaned of corrosion products by washing each coupon in a solution containing 50% NaOH and 100 g of zinc dust [24]. The coupons were then rinsed with running water and DDW, followed by washing with ethanol and acetone, and finally air-dried before being reweighed.
Corrosion rate (CR, $g \cdot m^{-2} \cdot h^{-1}$) and inhibition efficiency (IE, %) were calculated with equations 9-10 respectively:

$$CR\ (g \cdot m^{-2} \cdot h^{-1}) = \Delta m / Sxh \quad (9)$$

$$IE(\%) = (CR_0 - CR_i)x100 / CR_0 \quad (10)$$

where Δm – is the weight loss of carbon steel specimen (g) after the immersion period (h), CR_0 and CR_i represents the corrosion rate of carbon steel without and at present of the inhibitor, respectively. All measurements were performed in triplicate (n = 3), and the results are reported as mean values ± standard deviation (SD) at a confidence level of $\alpha = 0.95$.

RESULTS AND DISCUSSION

Qualitative phytochemical analysis
Aqueous extracts of various parts of *G.uralensis* and the whole plant were subjected to qualitative phytochemical screening. The plant samples collected in 2023 and 2024 were examined. The results are given in Table 1.
As can be seen, the phytochemical composition of *G. uralensis* for the years 2023 and 2024 has significant differences across various phytocomponents.

Table 1. Qualitative phytochemical analysis of *G.uralensis* aqueous extracts obtained in 2023, 2024

Phytocomponent (test, reagent)	2023					2024				
	Roots	Stems	Leaves	Inflorescences	Whole plant	Roots	Stems	Leaves	Inflorescences	Whole plant
Primary metabolites										
Carbohydrates (Molish's test)	+	++	-	+	++	+	++	-	+	++
Reducing sugars (Benedict's test)	++	-	+	++	++	++	-	+	++	++
Starch (Iodine test)	+	-	-	-	+	+	-	-	-	+
Proteins (Biuret test)	+	++	++	-	+	+	++	++	-	+
Amino acids (Ninhydrine test)	+	+	+	-	+	+	+	+	-	+
Gum (Shaking test)	+	++	+	++	+	+	++	+	++	+
Carboxylic acids ($NaHCO_3$)	+	++	+	-	+	+	++	+	-	+
Secondary metabolites										
Alkaloids (Dragendorf's test)	+++	+	+	++	+	+++	++	++	++	++
Phenols ($FeCl_3$)	+++	++	+	+	++	+++	++	+++	+++	+++
Flavonoids (Shinoda's test)	++	+++	+	+	++	+	+	+	++	++
Phlobatannins (1%HCl, boiling)	+	-	+	-	+	+	+	+	-	+
Saponins (Frothing test)	++	+	+	++	+	++	+	+	+	+
Steroids (Fluorescence test)	-	-	-	-	-	-	-	-	-	-
Xanthoproteins ($HNO_3 \rightarrow NH_4OH$)	+	++	+	+	+	+	++	-	-	+
Anthocyanins ($HCl \rightarrow NH_4OH$)	+++	++	++	++	++	+++	+	+	++	+
Leucoanthocyanins (*iso*-amyl alcohol)	-	-	+	++	+	-	-	++	+++	+

(+++) - highly present, (++) - moderately present, (+) - low present, (-) - absence.

Carbohydrates were moderately present in the roots in 2023 but showed a reduction to low levels in 2024, likely due to the flood's impact on carbohydrate synthesis or storage. In stems, carbohydrates were consistently present at low levels in both years. Reducing sugars, on the other hand, were highly present in roots across both years, indicating their resilience to environmental stress. Interestingly, reducing sugars in stems increased from low levels in 2023 to moderate levels in 2024, suggesting an adaptive response to the flood. Starch was present in roots in 2023 but was completely absent in 2024, likely reflecting the depletion of starch reserves under stress. Stems showed no presence of starch in either year. Proteins were highly present in roots in both years, demonstrating stability, whereas in stems, protein levels declined from moderate presence in 2023 to complete absence in 2024, indicating a higher sensitivity to flooding. Gum and carboxylic acids were moderately present in roots in 2023 but declined to low levels in 2024. In stems, these components remained stable at moderate levels across both years.

Across secondary metabolites, phenols were highly abundant in roots in both years, highlighting their resilience to environmental stress. Both years' moderate levels of phenols in stems demonstrated stability in spite of the flood. In roots, flavonoids decreased from moderate levels in 2023 to low levels in 2024, while in stems, they declined from high levels in 2023 to moderate levels in 2024. Anthocyanins were highly abundant in roots in both years, demonstrating their stability under stress. In stems, anthocyanins declined from moderate levels in 2023 to low levels in 2024, suggesting a greater vulnerability in stems. Saponins remained stable in both roots and stems, with moderate levels in roots and low levels in stems across both years. Steroids were consistently absent in both roots and stems in 2023 and 2024, indicating that they are not a significant component of *G. uralensis*. Leucoanthocyanins showed an interesting trend, with their presence increasing significantly post-flood. In roots, leucoanthocyanins were absent in 2023 but moderately present in 2024. In stems, they

increased from low levels in 2023 to high levels in 2024, suggesting an adaptive response to the environmental stress caused by the flood.

Results revealed that the heavy flood in 2024 had a mixed impact on the qualitative phytochemical composition of *G. uralensis*. Primary metabolites, such as carbohydrates and starch, showed a decrease in roots, while reducing sugars increased in stems, indicating an adaptive metabolic shift. Secondary metabolites, including phenols and anthocyanins, remained stable in roots, underscoring their resilience, whereas flavonoids and anthocyanins declined in stems, reflecting their sensitivity to environmental stress. Notably, leucoanthocyanins increased significantly in both roots and stems post-flood, suggesting a protective or adaptive role under adverse conditions. The results highlight that variations in both primary and secondary metabolites reflect the plant's adaptive responses to environmental stress.

Quantitative phytochemical screening

The comparative phytochemical analysis of *G.uralensis* parts aqueous extracts collected in 2023 and 2024 revealed pronounced changes in the accumulation of phenolic compounds and flavonoids following the severe flooding event of 2024 (Figure 2). Since both year samples were obtained from plants growing at the same place, the observed differences can be attributed primarily to environmental stress caused by prolonged waterlogging.

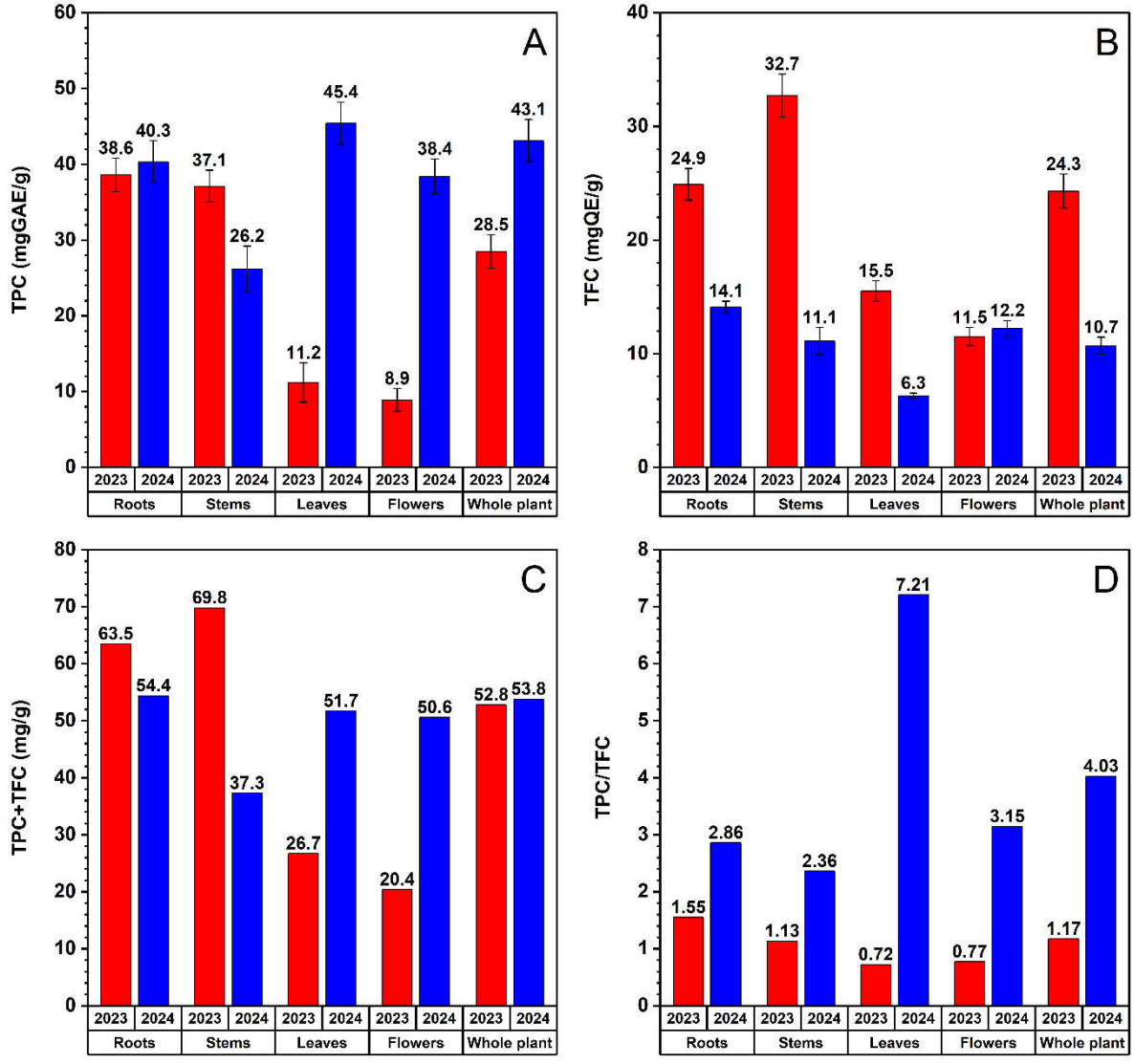

Fig. 2. Phytochemical composition of *G.uralensis* parts aqueous extracts: A – total phenolic content (TPC, mgGAE/g), B - total flavonoid content (TFC, mgQE/g), C – total content of phenols and flavonoids (mg/g), D – TPC/TFC ratio.

As shown in Figure 2A, the TPC increased notably in all plant parts after the flood. The largest increase was observed in leaves and flowers, where the TPC values rose from 11.2 to 26.2 and 8.9 to 28.4 mgGAE/g, respectively. In the roots, stems, and whole plant, TPC also increased moderately, reaching 40.3, 45.4, and 43.1 mg GAE/g in 2024. This general enhancement of phenolic levels suggests an activation of the phenylpropanoid pathway under stress conditions. Phenolic compounds are well recognized for their antioxidant properties and their ability to protect against oxidative damage, which commonly occurs under flooding and hypoxic stress conditions. Therefore, their accumulation likely represents a defensive metabolic response to excessive moisture and oxygen deprivation in the rhizosphere.

In contrast, the total flavonoid content (TFC) showed a strong decrease in 2024 across most plant parts (Figure 2B). The reduction was most significant in stems (from 32.7 to 11.1 mg QE/g) and leaves (from 15.5 to 6.3 mg QE/g). Only a slight increase was observed in flowers (from 11.5 to 12.2 mg QE/g). This trend suggests that flooding conditions may have suppressed flavonoid biosynthesis or accelerated flavonoid degradation, possibly due to inhibited photosynthesis and lower light intensity during waterlogging. Flavonoids, being secondary metabolites associated with UV protection and pigmentation, are highly sensitive to environmental cues such as light and oxygen availability; their decrease indicates a shift in metabolic priorities toward simpler phenolic antioxidants.

The total content of phenolics and flavonoids (TPC + TFC) remained relatively stable between the two years (Figure 2C), with only minor variations across plant parts. This indicates that although the qualitative composition of secondary metabolites changed, the total metabolic investment in phenolic-type compounds was maintained. Such stability suggests that *G.uralensis* compensates for the loss of certain metabolites by redirecting biosynthetic fluxes within the phenylpropanoid pathway, maintaining overall antioxidant potential despite stress.

A particularly informative parameter is the TPC/TFC ratio (Figure 2D), which reflects the relative contribution of general phenolics to flavonoids. This ratio increased sharply in 2024, especially in leaves (from 0.72 to 7.21) and in the whole plant (from 1.17 to 4.03). The elevated ratio demonstrates a clear metabolic shift toward the accumulation of non-flavonoid phenolic compounds which are more directly involved in oxidative stress defense. This transformation highlights the biochemical plasticity of licorice, allowing it to adjust its metabolic profile to counteract the detrimental effects of flooding.

In summary, the flood-induced stress in 2024 led to substantial reorganization of the phenolic metabolism in *G.uralensis*. The increase in TPC accompanied by a decrease in flavonoids and a higher TPC/TFC ratio suggests activation of protective antioxidant mechanisms, particularly in the aerial parts of the plant. These findings confirm that *G.uralensis* responds to hydrological stress by enhancing phenolic antioxidant defenses while modulating the synthesis of specific flavonoid compounds, reflecting an adaptive strategy for maintaining redox balance and metabolic stability under extreme environmental conditions.

Antioxidant activity

The antioxidant activity of *G.uralensis* parts aqueous extracts was estimated by several complementary assays reflecting different mechanisms of free radical scavenging and shown in Figure 3.

The obtained results clearly demonstrate that the flooding in 2024 markedly affected the redox behavior of the extracts, enhancing the antioxidant potential of most plant parts.

In the total antioxidant capacity (TAC, Figure 3A) assay, all plant parts collected in 2024 exhibited higher activity compared with the pre-flood samples. The most pronounced increase occurred in roots (from 2.29 to 2.98 mmol AA/g) and in the whole plant (from 1.87 to 2.72 mmol AA/g), whereas smaller increases were observed in stems, leaves, and flowers. The elevated TAC values correspond well with the higher total phenolic content (TPC) detected in 2024 and indicate the accumulation of reducing agents capable of electron donation. Flood-induced oxidative stress likely stimulated the biosynthesis of phenolic antioxidants, contributing to the enhanced overall reducing capacity.

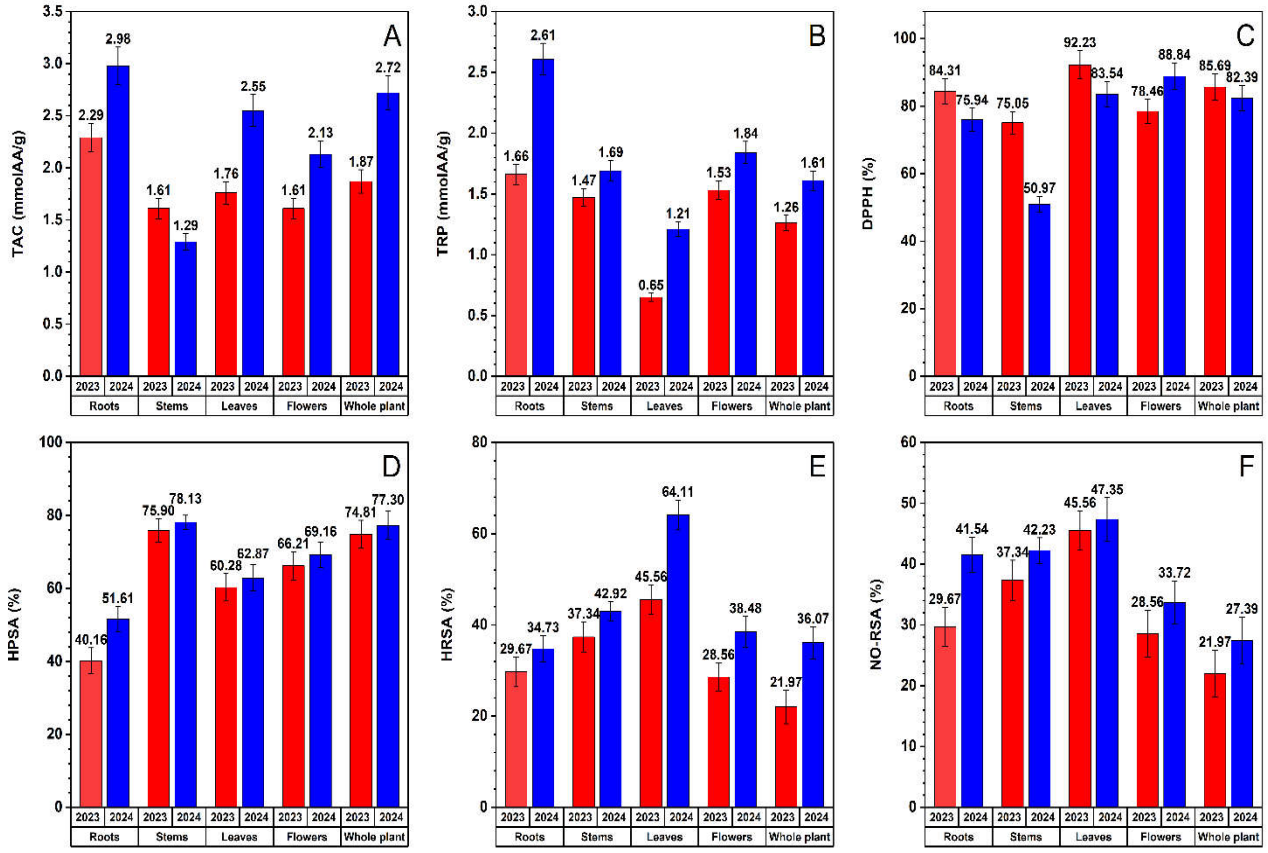

Fig. 3. Total antioxidant activity (TAC) (A), total reducing power (TRP) (B) and activity of *G.uralensis* parts aqueous extracts to scavenge DPPH-radicals (C), hydrogen peroxide (HPSA) (D), OH-radicals (HRSA) (E), and NO-radicals (NO-RSA) (F) at concentration of 1.0 mg/mL.

Similarly, total reducing power (TRP, Figure 3B) showed a steady increase in all plant parts after flooding, with roots and leaves showing the largest increases (1.66 to 2.61 and 0.65 to 1.69 mmol AA/g, respectively). This rise reflects the abundance of phenolic hydroxyl groups able to reduce Fe^{3+}/Fe^{2+} or similar electron-accepting species, again supporting the activation of antioxidant metabolism under stress conditions.

The DPPH radical scavenging activity (Figure 3C), which measures the ability to neutralize stable free radicals, revealed a more variable pattern. After the flood, the scavenging activity slightly decreased in roots (from 84.31% to 75.94%) and in leaves (from 92.23% to 83.54%), whereas it remained relatively stable or slightly higher in stems, flowers, and the whole plant. Despite these minor declines, all samples retained very high activity (>70%), confirming strong intrinsic radical-scavenging potential. The modest decrease in some organs may be associated with compositional changes - specifically, the decline in flavonoid content observed in 2024 - which could have altered the radical-quenching efficiency despite an overall increase in phenolics.

In contrast, the hydrogen peroxide scavenging activity (HPSA, Figure 3D) increased sharply in 2024 for all plant parts, particularly in roots (from 40.16% to 51.61%) and stems (from 75.90% to 78.13%). This suggests that waterlogging stress enhanced the enzymatic and non-enzymatic antioxidant systems responsible for detoxifying reactive oxygen species such as H_2O_2.

A more pronounced enhancement was detected in the hydroxyl radical scavenging activity (HRSA, Figure 3E). In 2024, HRSA values increase in leaves (from 42.56% to 64.11%) and moderately in other parts, reflecting a stronger ability to neutralize highly reactive hydroxyl radicals generated under oxidative stress. This effect further supports the view that the phenolic metabolism of *G.uralensis* was upregulated in response to flooding, leading to improved reactive oxygen species (ROS) scavenging efficiency.

Moreover, the nitric oxide radical scavenging activity (NO-RSA, Figure 3F) also increased in 2024 for most plant parts, especially in roots (from 29.67% to 41.54%). Since nitric oxide is a reactive

signaling molecule involved in stress responses, its enhanced scavenging indicates that post-flood *G.uralensis* plants developed a more effective defense system to control nitrosative stress.

All antioxidant assays consistently demonstrated that flooding stress in 2024 stimulated antioxidant activity in *G. uralensis*, though with some differences among plant organs. Roots, stems, and leaves exhibited the most pronounced responses, indicating that these tissues play a key role in maintaining redox homeostasis under excess water conditions. The observed increases in TAC, TRP, HPSA, HRSA, and NO-RSA, along with relatively stable DPPH values, reflect both a quantitative enhancement of total antioxidant capacity and a qualitative adaptation of radical-scavenging mechanisms.

When considered alongside the phytochemical data, these findings confirm that flood-induced environmental stress activated antioxidant metabolism in *G. uralensis*, primarily through the accumulation of phenolic and non-flavonoid compounds possessing strong reducing and radical-scavenging abilities. The coordinated increase in multiple antioxidant indices highlights biochemical adaptability of licorice, which strengthens its oxidative defense network to endure extreme hydrological disturbances.

Sun protection factor (SPF) and photostability determination

The absorbance values determined by UV-Vis spectra were used to calculate the SPF according to equation (6). Figure 4 shows the SPF of freshly prepared ethanolic solutions of *G.uralensis* parts aqueous extracts in two year comparisons, as well as the SPF of these extracts after 6 weeks of exposure to direct sunlight and in the dark with photostability and photosensitivity.

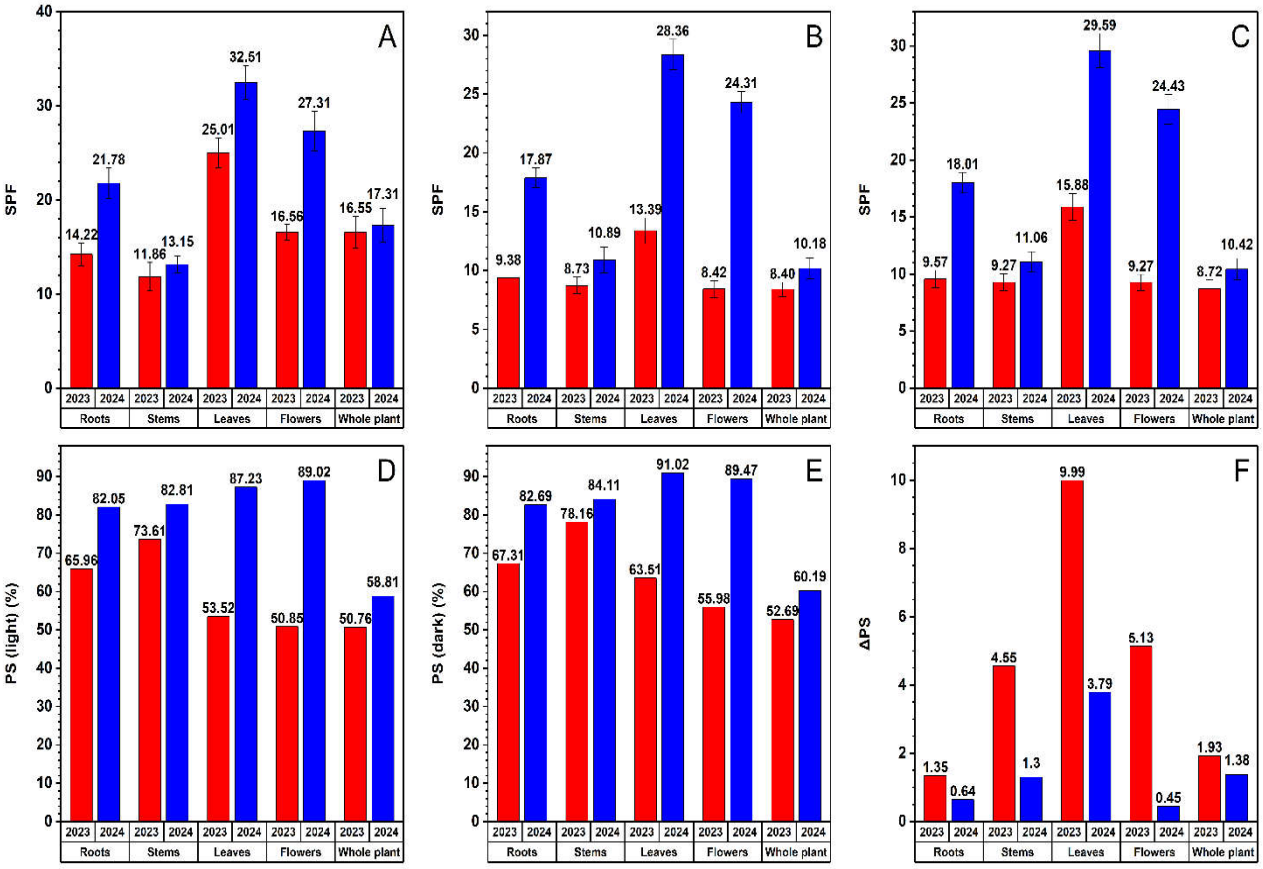

Fig. 4. Sun protection factor (SPF) of *G. uralensis* aqueous extracts (1.0 g/L): freshly prepared ethanol solutions (A); after six weeks of exposure to direct sunlight (B) and in the dark (C); photostability under sunlight (D) and in the dark (E); and photosensitivity (F).

Figure 4 presents the comparative photoprotective efficiency of aqueous extracts of *G. uralensis* (1.0 g/L) collected in 2023 and 2024. The SPF of freshly prepared ethanolic solution of extracts (Fig. 4A) demonstrated significant interannual and interpart variability. Extracts from 2024 showed

consistently higher SPF values than those from 2023, with the leaves exhibiting the highest SPF (32.51), followed by flowers (27.31) and stems (25.01), while roots and whole-plant extracts showed more moderate activity (21.78 and 17.31, respectively).
After six weeks of sunlight exposure (Figure 4B), all samples experienced a decrease in SPF, indicating partial photodegradation of UV-absorbing compounds. Nevertheless, the 2024 leaf extract retained a relatively high SPF (28.36), confirming its superior photostability. Samples stored in the dark (Fig. 4C) demonstrated less pronounced losses, supporting the hypothesis that the reduction in SPF under sunlight is primarily due to photolytic rather than oxidative processes.
Photostability determination (Figures 4D–E) corroborate these findings: leaf and flower extracts from 2024 exhibited the highest preservation of SPF under sunlight (87÷89%) and in the dark (84÷91%), while 2023 samples showed notably lower stability. The photosensitivity index (ΔPS, Figure 4F) was lowest for leaf and flower extracts, suggesting that polyphenolic constituents in these organs provide enhanced UV resistance and molecular stability.
The results confirm that extracts obtained after flooding (2024) possess markedly improved photoprotective and photostability properties. This enhancement may be attributed to the stress-induced accumulation of UV-absorbing flavonoids and other phenolic compounds, which increase both the SPF value and the long-term stability of the formulations.
Earlier it was noted that roots are traditionally the most potent parts of *Glycyrrhiza* species due to their high concentrations of flavonoids and saponins, which have well-documented antioxidant and photoprotective properties [25].

Corrosion inhibition properties.
The inhibition efficiency (IE%) of *G. uralensis* extracts against carbon steel corrosion was assessed in 0.5M H_2SO_4 and 3% NaCl solutions for samples collected before (2023) and after (2024) the flooding event. Results are shown in Figure 5.

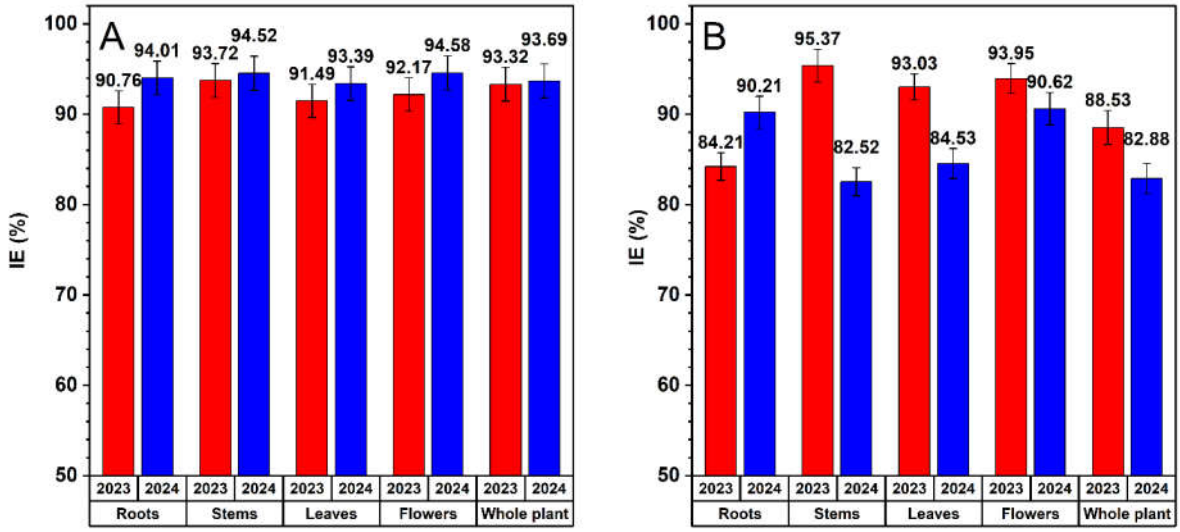

Fig. 5. Inhibition efficiency of *G. uralensis* aqueous extracts on carbon steel in 0.5M H_2SO_4 (A) and 3% NaCl (B) at 1.0 g/L for 18h of immersion.

In acidic medium (Figure 5A), all parts of *G. uralensis* demonstrated high inhibition efficiencies (90.7–94.6 %), indicating effective adsorption of phytocomponents on the carbon steel surface. Following the 2024 flooding, a slight but consistent increase in efficiency was observed across all plant parts, most notably in roots (from 90.8 % to 94.0 %) and flowers (from 92.2 % to 94.6 %). This enhancement is attributed to the increased proportion of flavonoid constituents in post-flood samples, whose planar, π-conjugated structures and electron-donating heteroatoms facilitate strong chemisorptive interactions with the metal surface. Such molecular features promote the formation of compact protective films, effectively suppressing both anodic and cathodic corrosion reactions in acidic environments.

On the other hand, under neutral chloride conditions (3% NaCl), inhibition efficiencies decreased markedly after the flood, ranging from 82.5 to 90.6 %, compared with 84.2÷95.4 % in 2023. The decrease was most pronounced for stem (95.4 → 82.5 %) and whole plant (88.5 → 82.9 %) extracts. These results suggest that flooding altered the hydrophilic–lipophilic balance of extractable metabolites, diminishing their adsorption affinity in neutral media where hydrogen bonding and electrostatic interactions dominate. The reduction in total phenolic content, accompanied by a relative increase in less polar flavonoids, likely weakened the stability of adsorbed layers on hydrated steel surfaces.

In light of these observations, flooding can be regarded as a factor that selectively altered the phytochemical profile of *G. uralensis*, increasing the abundance of nonpolar flavonoids at the expense of phenolic constituents. This composition change increased inhibition efficiency in strongly acidic media through the interaction of the π-donor, but decreased protection in chloride-containing media, which is dependent on physical adsorption. These findings highlight the environmentally responsive nature of plant-derived inhibitors and the crucial role of molecular polarity and aromaticity in defining corrosion protection performance.

Correlations of phytochemical composition and functional properties of G. uralensis aqueous extracts

Figure 6 presents the Pearson correlation matrices for the phytochemical composition and functional properties of *G. uralensis* aqueous extracts obtained before and after flooding. The results clearly demonstrate substantial shifts in the interrelations between the studied variables, reflecting strong environmental modulation of the plant's metabolic system.

In 2023 (pre-flood conditions, Figure 6A), a high degree of positive correlation was observed between TPC and TFC ($r = 0.999$), as well as between TPC/TFC and TAC, DPPH, and HRSA activities. These relationships indicate that phenolics and flavonoids were the main contributors to the antioxidant potential of the extracts. Similarly, significant positive correlations between antioxidant indices and inhibition efficiency (IE) in both 0.5 M H_2SO_4 and 3 % NaCl media suggest that electron-donating and radical-scavenging capacities of polyphenols played an essential role in the corrosion protection mechanism. Strong correlations between SPF and antioxidant parameters ($r > 0.9$) further highlight the multifunctionality of phenolic compounds as universal UV absorbers and redox-active agents.

In contrast, the post-flood samples (2024, Figure 6B) exhibited a noticeable alteration in the correlation pattern. Several relationships either weakened or reversed - for example, correlations between TPC and inhibition efficiency, SPF, and photostability parameters became negative or statistically insignificant. This inversion suggests that under flooding stress, the compositional profile of the phenolic fraction and its functionality changed substantially. Flooding likely induced anaerobic metabolism, oxidative stress, and altered phenylpropanoid biosynthesis, leading to the accumulation of noncanonical phenolics, isoflavones, or stress-related metabolites (e.g., glycosides, saponins) that may possess weaker electron-donating but stronger UV-absorbing or protective properties. As a result, the direct linear relationships between phenolic content and functional properties became less pronounced or even opposite.

The observed reversal of correlations can also be explained by the shift in extract composition balance: while TPC increased quantitatively after flooding, their qualitative composition (hydroxylation pattern, conjugation degree, and solubility) may have changed. Some metabolites might have acted as competitive adsorbates on the metal surface or undergone photochemical degradation under UV exposure, decoupling the previous positive synergy among antioxidant, photoprotective, and anticorrosive functions.

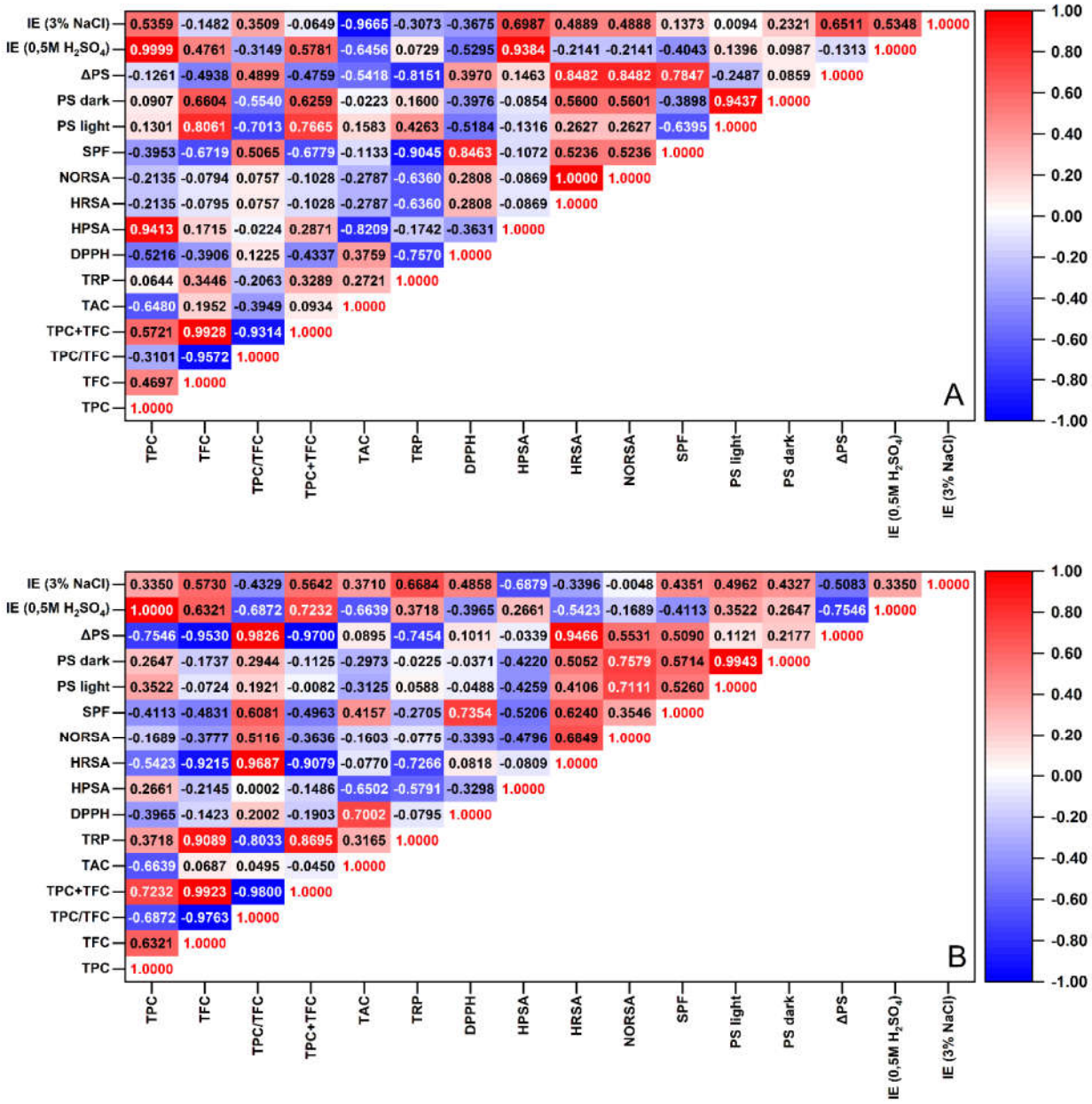

Fig. 6. Pearson correlation analysis for phytochemical composition and functional properties of *G. uralensis* aqueous extracts for 2023 (A) and 2024 (B).

Correlation analysis shows that flood stress not only altered the total phytochemical concentration but also rearranged functional relationships between classes of biochemicals and their activity profiles. These findings emphasize that environmental perturbations can substantially reshape the multifunctional behavior of *G. uralensis*, transforming it from a system dominated by polyphenolic synergy in 2023 into one characterized by more complex and, in some cases, antagonistic interactions in 2024.

The correlation patterns obtained between phytochemical composition and the functional properties of *G. uralensis* aqueous extracts reflect the shared chemical principles underlying antioxidant, photoprotective, and anticorrosive activities. Under normal growth conditions, strong positive correlations were observed among TPC, TFC, antioxidant assays (DPPH, ABTS, FRAP), and SPF. These relationships indicate that the same polyphenolic compounds are primarily responsible for both radical-scavenging and UV-absorbing effects. Phenolic hydroxyl groups and conjugated aromatic systems effectively donate electrons or hydrogen atoms to neutralize free radicals, while their extended π-conjugation allows absorption of harmful UV radiation, preventing photooxidative

degradation. Therefore, the high correlation between antioxidant capacity and SPF reflects a dual-function mechanism where the electronic structure of phenolic molecules ensures simultaneous redox stabilization and UV screening. Moreover, moderate to strong correlations between antioxidant indices and corrosion inhibition efficiency suggest that the electron-donating ability of phenolics also facilitates their adsorption onto metal surfaces. Through π–d interactions and coordination via oxygen atoms, these molecules form protective films that block aggressive ions and suppress anodic and cathodic reactions. The positive correlation between inhibition efficiency and antioxidant activity thus reflects a shared mechanism based on charge transfer and surface passivation processes.

After flooding, many of these correlations were weakened or reversed. This shift indicates that the plant's metabolic adaptation under stress led to a compositional change in its polyphenolic profile. Flooded plants accumulated higher amounts of modified flavonoids, glycosylated derivatives, and stress-related phenolic acids that differ in solubility, conjugation, and reactivity. Some of these compounds may possess stronger UV absorption but lower surface adsorption capacity, or *vice versa*, resulting in the partial decoupling of antioxidant, photoprotective, and anticorrosive behaviors. In essence, flooding triggered a reallocation of metabolic resources toward the biosynthesis of specialized metabolites with more selective functions rather than broad multifunctionality.

The observed reversal of correlations emphasizes that multifunctionality in *G. uralensis* is highly dependent not only on TPC but also on the qualitative nature of these metabolites—their oxidation potential, aromaticity, and molecular geometry. Compounds with higher conjugation and lower ionization potential are more efficient as antioxidants and UV absorbers, while those with planar aromatic structures and polar substituents favor adsorption on metal surfaces, enhancing corrosion inhibition. Thus, the flood-induced restructuring of metabolic pathways modulated the balance between these properties, providing valuable insight into how environmental stress shapes the functional chemistry of medicinal plants and the protective properties of plant extracts.

CONCLUSIONS

This study demonstrates that severe flooding serves as a powerful environmental trigger, profoundly altering the secondary metabolite composition of *G. uralensis* and, consequently, its multifunctional properties. The metabolic shift, marked by an increase in total phenolics and a relative decreade in flavonoids, reflects an adaptive response to hypoxic and oxidative stress aimed at maintaining redox balance. Correlation analysis revealed that flooding disrupted the integrated functional network characteristic of the pre-flood state (2023), where strong positive associations among phytochemical content, antioxidant activity, photoprotection, and corrosion inhibition suggested a unified polyphenol-driven mechanism. Nevertheless, post-flood samples (2024) exhibited weakened or inverted correlations, indicating a reallocation of metabolic resources toward the synthesis of specialized stress-related compounds with narrower functional spectra. This transformation was mirrored in the anticorrosion behavior - enhanced efficiency in acidic media due to increased nonpolar flavonoids facilitating chemisorption, but reduced protection in neutral environments where physical adsorption predominates. From an applied perspective, post-flood extracts, particularly from aerial parts, represent valuable sources of stress-induced antioxidant and photoprotective agents with potential cosmetic and pharmaceutical applications. In summary, these findings offer an important framework for understanding how extreme hydrological conditions, increasingly frequent under climate change, modulate the biochemical composition and practical utility of medicinal plants.

ACKNOWLEDGEMENTS

The authors gratefully acknowledge the head and staff of the Laboratory of Ecology and Biogeochemistry of M. Utemisov West Kazakhstan University for providing the necessary facilities, technical support, and assistance to conduct this research.

REFERENCES

[1] JIANG, L., AKRAM, W., LUO, B., HU, S., FARUQUE, M.O., AHMAD, S., YASIN, N.A., KHAN, W.U., AHMAD, A., SHIKOV, A.N., CHEN, J., HU, X. Front. Pharmacol., **12**, 2021, https://doi.org/10.3389/fphar.2021.658670.
[2] LIAO, M., ZHAO, Y., HUANG, L., CHENG, B., HUANG, K. RSC Adv. **6,** no. 89, 2016, p. 86640, https://doi.org/10.1039/C6RA17770K.
[3] HAYASHI, H., ZHANG, S.-L., NAKAIZUMI, T., SHIMURA, K., YAMAGUCHI, M., INOUE, K., SARSENBAEV, K., ITO, M., HONDA, G. Chem. Pharm. Bull. **51,** no. 10, 2003, p. 1147, https://doi.org/10.1248/cpb.51.1147.
[4] UZAKBAY, G., ISSAGAT, R., MENDIGALIYEV, Y., MAKSOTOVA, A., AKATYEV, N. Bulletin WKU, **1**, no. 97, 2025, p. 549, https://doi.org/10.37238/2960-1371.2960-138X.2025.97(1).44.
[5] KURZAWA, M., WILCZYŃSKA, E., BRUDZYŃSKA, P., SIONKOWSKA, A. Cosmetics, **9**, no. 6, 2022, p. 134, https://doi.org/10.3390/cosmetics9060134.
[6] NUNES, A.R., RODRIGUES, A.L.M., DE QUEIRÓZ, D.B., VIEIRA, I.G.P., NETO, J.F.C., JUNIOR, J.T.C., TINTINO, S.R., DE MORAIS, S.M., COUTINHO, H.D.M., J. Photochem. Photobiol. B: Biol., **189,** 2018, p. 119, https://doi.org/10.1016/j.jphotobiol.2018.10.013.
[7] FERREIRA JÚNIOR, J.M., DE VASCONCELOS SILVA, M.G., MONTEIRO, J. A., BARROS, A. DE S., FALCÃO, M.J.C., DE MORAIS, S.M., Int. J. Electrochem. Sci., **11**, 2016, p. 3862, https://doi.org/10.20964/110388.
[8] VOROBYOVA, V., SKIBA, M., SHAKUN, A., NAHIRNIAK, S., Int. J. Corros. Scale Inhib, **8**, no. 2, 2019, p. 150, https://doi.org/10.17675/2305-6894-2019-8-2-1.
[9] BANU, K. S., CATHRINE, L., Int. J. Adv. Res. Chem. Sci., **2**, no. 4, 2015, p. 25.
[10] BALAMURUGAN, V., FATIMA M.A., S., VELURAJAN, S., Int. J. Adv. Res. Innov. Ideas Educ. **5**, no. 1, 2019, p. 236.
[11] MAKSOTOVA, A., ISSAGAT, R., NURZHANOVA, D., AKATYEV, N. Eur. J. Biol., **81**, no. 1, 2025, p. 72, https://doi.org/10.26650/EurJBiol.2025.1634853.
[12] SINGLETON, V. L., ROSSI, J. A., JR, J., Am. J. Enol. Vitic., **16**, 1965, p. 144.
[13] ZHISHEN, J., MENGCHENG, T., JIANMING, W. Food Chem., **64**, no. 4, 1999, p. 555.
[14] SAEED, N., KHAN, M.R., SHABBIR, M., BMC Complement. Altern. Med., 12, 2012, p. 221. https://doi.org/10.1186/1472-6882-12-221.
[15] HINNEBURG, I., DORMAN, H.J.D., HILTUNEN, R., Food Chem., **97**, no. 1, 2006, p. 122. https://doi.org/10.1016/j.foodchem.2005.03.028.
[16] BRAND-WILLIAMS, W., CUVELIER, M.E., BERSET, C., Food Sci. Technol., **28**, no. 1, 1995, p. 25.
[17] MUKHOPADHYAY, D., DASGUPTA, P., SINHA ROY, D., PALCHOUDHURI, S., CHATTERJEE, I., ALI, S., GHOSH DASTIDAR, S. Free Radic. Antioxid., **6**, no. 1, 2016, p. 124, https://doi.org/10.5530/fra.2016.1.15.
[18] GOVINDAN, P., MUTHUKRISHNAN, S., J. Acute Med., **3**, no. 3, 2013, p. 103, https://doi.org/10.1016/j.jacme.2013.06.003.
[19] HAZRA, B., BISWAS, S., MANDAL, N. BMC Complement. Altern. Med., **8**, no. 63, 2008, https://doi.org/10.1186/1472-6882-8-63.
[20] SREEJAYAN, RAO M.N., J. Pharm. Pharmacol., **49**, no. 1, 1997, p. 105, https://doi.org/10.1111/j.2042-7158.1997.tb06761.x.
[21] MANSUR, J., BREDER, M., MANSUR, M., AZULAY, R., An. Bras. Dermatol., **61**, 1986, p. 121.
[22] SAYRE, R., AGIN, P., LEVEE, G., MARLOWE, E. Photochem. Photobiol., **29**, 1979, p. 559.
[23] AKATYEV, N., SAMIGOLLA, A., Prosp. Pharm. Sc., **22**, no. 4, 2024, p. 160, https://doi.org/10.56782/pps.285.
[24] ISO 8407:2021. Corrosion of Metals and Alloys, Removal of corrosion products from corrosion test specimens.

[25] CERULLI, A., MASULLO, M., MONTORO, P., PIACENTE, S., Cosmetics, **9**, no. 1, 2022, https://doi.org/10.3390/cosmetics9010007.

Citation: Uzakbay, G., Akatyev, N., Impact of flooding on the multifunctionality of Glycyrrhiza uralensis: a comparative study of phytochemical, antioxidant, anticorrosion, and photoprotective activities, *Rom. J. Ecol. Environ. Chem*., **2025**, 7, no.2, pp. 52÷67.